



# Interlaboratory Reproducibility of Contour Method Data in a High Strength Aluminum Alloy

C. R. D'Elia<sup>1</sup> · P. Carlone<sup>2</sup> · J. W. Dyer<sup>3</sup> · J. B. Lévesque<sup>4</sup> · J. Araújo de Oliveira<sup>5</sup> · M. B. Prime<sup>3</sup> · M. J. Roy<sup>6</sup> · T. J. Spradlin<sup>7</sup> · R. Stilwell<sup>8</sup> · F. Tucci<sup>2</sup> · A. N. Vasileiou<sup>6</sup> · B. T. Watanable<sup>9</sup> · M. R. Hill<sup>1</sup>

Received: 3 February 2022 / Accepted: 5 April 2022 / Published online: 25 April 2022  
© The Author(s) 2022

## Abstract

**Background** The contour method for residual stress measurement has seen significant development, but an experimental reproducibility study utilizing physical samples has not been published.

**Objective** A double-blind reproducibly study is reported, having scope beginning with EDM cutting and ending with residual stress calculation.

**Methods** A reinforced I-beam sample geometry is identified for its unique residual stress profile when extracted from residual stress bearing quenched aluminum bar (7050-T74). Contour measurements are prescribed on a midplane of symmetry with dimensions 24.0 mm by 50.0 mm. Fourteen identically prepared samples are fabricated from a single long bar with well characterized and uniform residual stress. Five samples throughout the bar are identified for planning measurements to validate sample uniformity and overall suitability of the residual stress field. The planning measurements employ a range of techniques: contour method, neutron diffraction, and hole-drilling. Eight samples are distributed to an international group of participants to execute their standard measurement practice. A double-blind process is followed to provide anonymity.

**Results** Results are provided by eight participants: six being self-similar and two being quite different, the latter set aside as outliers. An average residual stress field is established from non-outlying results and the spatial distribution of reproducibility standard deviation is determined. The average stress field ranges from -60 to 70 MPa and the reproducibility standard deviation averages 8.1 MPa on the measurement plane. The average reproducibility standard deviation is about 3 × larger for points within 1.0 mm of plane boundaries (17.6 MPa) than for the remaining points (6.1 MPa).

**Conclusions** Reproducibility standard deviation (among different labs) for contour method residual stress measurement is found to be very similar to repeatability standard deviation (in a single lab) reported in prior work. The reproducibility observed here, for the entire measurement process, is also similar to that found in a prior reproducibility study limited to contour method data analysis.

**Keywords** Contour method · Residual stress · Reproducibility · Precision · Uncertainty

✉ C. R. D'Elia  
crdelia@ucdavis.edu

<sup>1</sup> University of California, Davis, CA 95616, USA

<sup>2</sup> University of Salerno, Fisciano, SA, Italy

<sup>3</sup> Los Alamos National Laboratory, Los Alamos, NM 87545, USA

<sup>4</sup> Hydro-Québec Research Institute, Varennes (Québec) J3X 1S1, Canada

<sup>5</sup> StressMap – The Open University, Milton Keynes MK7 6AA, UK

<sup>6</sup> University of Manchester, Manchester M1 3BU, UK

<sup>7</sup> Air Force Research Laboratory, United States Air Force, Wright-Patterson, AFB, OH 45433, USA

<sup>8</sup> Boeing Co, Seattle, WA 98108, USA

<sup>9</sup> Hill Engineering, LLC, Rancho Cordova, CA 95670, USA



## Introduction

The present study develops data on reproducibility of contour method residual stress measurements. The contour method was first developed by Prime circa 1999 and first published in 2001 [1]. The method produces a two-dimensional map of residual stress normal to a plane of interest in a workpiece and is typically applied at a plane of symmetry. In the time since the method was first developed, a great number of contour measurements have been published in metallic materials with residual stress from a wide range of sources including welding, quenching, additive manufacturing, hole cold working, laser shock peening, among others [2, 3]. Additional efforts have investigated measurement repeatability and uncertainty within an individual laboratory [4–6].

This work is an extension of a recent collaborative, inter-laboratory effort [7] to quantify contour method reproducibility. While the scope of the prior effort was limited to data analysis and stress calculation, this work encompasses the complete measurement and analysis process. The present effort is carried out by an international working group drawn from nine organizations with points of contact being:

- Michael R. Hill & Christopher D’Elia – University of California – Davis
- Michael B. Prime – Los Alamos National Laboratory
- Pierpaolo Carlone – University of Salerno
- Jean-Benoît Lévesque – Hydro-Québec Research Institute
- Jeferson Araujo de Oliveira – StressMap
- Thomas J. Spradlin – United States Air Force – Air Force Research Laboratory
- Richard Stilwell – Boeing Co.
- Anastasia Vasileiou – University of Manchester
- Brett T. Watanabe – Hill Engineering, LLC

UC Davis organized the effort and designed and manufactured samples. The working group agreed to follow a double-blind protocol to preserve anonymity of each participant and encourage open discussion of the experimental data. Only UC Davis had prior knowledge of the source of the residual stress field; each participant only had knowledge of their specific result.

## Methods

### Contour Method

The present study provides measurement reproducibility for the contour method. The contour method has five main steps [2, 8]:

1. identifying a plane of interest in the workpiece
2. cutting along the plane of interest to release residual stress using wire electrical discharge machining (EDM)
3. measurement of the topography (surface form) of the cut surfaces
4. data processing of the surface topography (screening, aligning, filtering, smoothing, averaging), and
5. calculation of the residual stresses by linear elastic stress analysis

While the scope of the prior study [7] was limited to steps four and five, the present study encompasses all steps.

### Roles and Procedures

A series of roles maintain the anonymity of results within the working group and the integrity of the double-blind study. The *fabricator* role designs, produces, and verifies the samples used in the study and is assumed by Hill and D’Elia. Excluding UC Davis, all organizations make measurements for the interlaboratory reproducibility study and hold the *participant* role. The participants are provided samples but are unaware of the residual stress designed into the samples or the source of that residual stress field. The *distributor* receives samples from the *fabricator* and distributes one to each *participant* for measurement. The *distributor* is blind to the sample identification and randomizes the samples sent to *participants*. The *collector* role collects the measurement data from the *participants* in encrypted files and anonymously delivers those files to the *analyst*. A third party (Jeffrey Bunch, known to many of the working group) serves the *distributor* and *collector*. The *analyst* is able to decrypt the encrypted files and receives data corresponding to each sample but is blind to which *participant* performed each measurement. Hill and D’Elia also act in the *analyst* role.

### Material and Sample Configuration

Samples are machined by the fabricator from a single aluminum alloy (AA7050-T74) residual stress bearing bar. The bar is saw cut from larger 50.8 mm nominal thickness AA7050-T7451 plate with the rolling (L) direction along the 914 mm length of the bar. The bar cross section is 50.8 mm thick (ST) by 76.3 mm wide (LT). Residual stress is created in the bar by solution heat treatment followed by warm water quench and two-stage artificial aging. The heat treatment process follows specification AMS 2770H, which provides the T74 temper. Sample material removed from the center section of the long bar contains residual stress invariant along the bar length, as to be expected from quenching and found in prior work [9].



The reinforced I-beam sample geometry shown in Fig. 1 is chosen by the fabricator, having overall dimensions of 50.0 mm × 75.0 mm × 24.0 mm. The specific geometry is selected based on finite element (FE) analyses for a small number of preliminary sample configurations that provide estimated residual stress fields from prior measurements of triaxial residual stress determined in a replicate bar [9]. Preliminary sample configurations considered included perturbations of the I-beam web, flange, and stiffener dimensions. The I-beam geometry has web and flange thicknesses of 8.0 mm and 6.0 mm respectively. A tapered central stiffener provides a symmetry plane (section A-A in Fig. 1) for contour measurement. A pair of 6.0 mm cross-drilled holes, introduced into the sample adjacent to the measurement plane, serve to localize and add complexity to the residual stress distribution. The I-beam section and cross-drilled holes provide (according to the FE estimate) a somewhat more complicated, two-dimensional residual stress distribution when compared to the bent-beam configuration used in the prior reproducibility study [7].

A total of 14 samples are extracted from the residual stress bearing bar and numbered sequentially along the length as CMRE-A-00 through CMRE-A-13. Material at each end of the bar is discarded, 157.0 mm at the end toward CMRE-A-00 and 100.0 mm at the end opposite. Samples

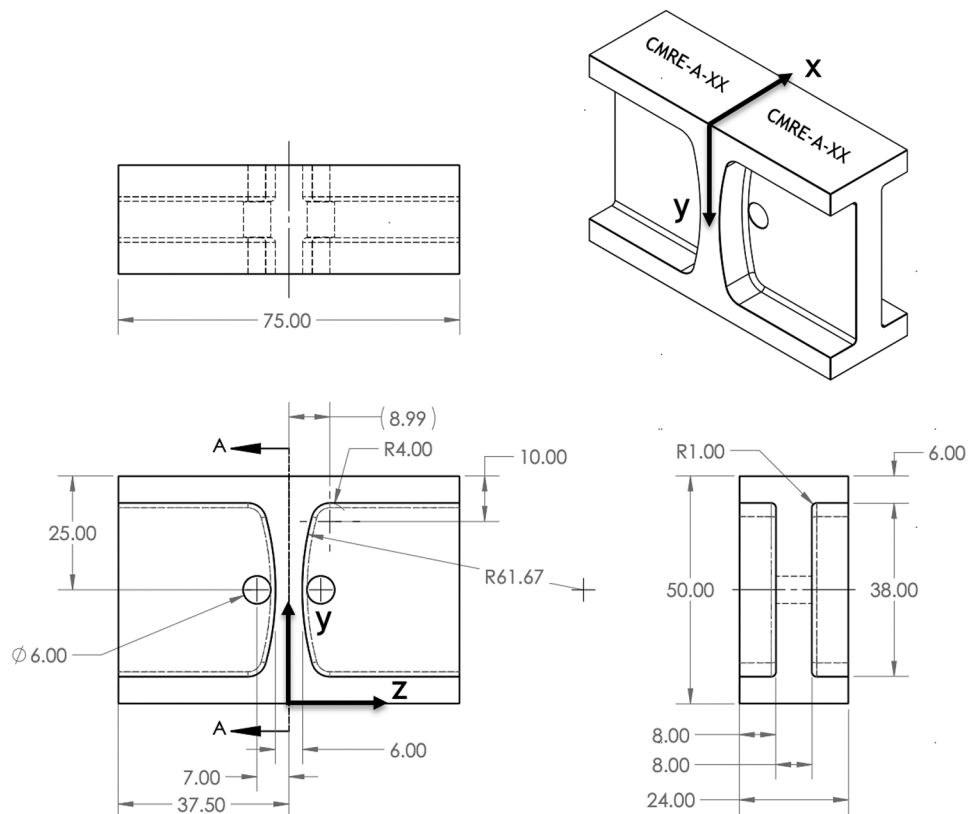
nearest each end of the bar and near the center are allocated to planning measurements, eight other samples are allocated to participant measurements, and one sample was held in spare. Samples are identified with A## to indicate sample CMRE-A-## (where ## is 00, 01, ..., 13).

### Planning Measurements

Planning residual stress measurements are conducted by the fabricator in three samples (A01, A07, and A13) using the contour method, one sample (A08) using neutron diffraction, and one sample (A00) using hole-drilling. The planning measurements confirm the suitability of the residual stress distribution and consistency of samples with position along the length of the parent bar.

Contour planning measurements in A01, A07, and A13 follow typical practice reported in prior work [1, 2, 4, 8]. EDM cutting is performed with 0.25 mm brass wire after carefully clamping the workpiece. Filler material (also called sacrificial material), comprising 5.0 mm thick aluminum sheet, is clamped on all four boundaries of the cut plane to mitigate potential errors from typical EDM-induced artifacts [2, 10]. The topography of each cut surface is measured using a scanning laser profilometer at a grid of points with 0.25 mm spacing. The data from the two cut surfaces are

**Fig. 1** Sample geometry, coordinate system, and specified EDM cutting direction (dimensions in mm)



averaged and the average smoothed using bivariate splines. Residual stress is calculated from a linear elastic stress analysis in ABAQUS using a mesh with 492,883 quadratic tetrahedral elements (C3D10) and properties for AA7057T74,  $E = 71.7$  GPa and  $\nu = 0.33$ .

Hole-drilling planning measurements are made in A00 at the mid-length of the top ( $Y = 0$  mm; coordinates shown in Fig. 1) and bottom ( $Y = 50.0$  mm) edges of the measurement plane to indicate the near-surface residual stress. Hole-drilling is performed according to ASTM E837 [11] using a 2.0 mm diameter hole drilled at the center of a three-axis strain gage rosette in 0.05 mm depth increments to a final depth of 1.0 mm. At each depth increment, the redistribution of residual stress is indicated by three changes of strain. Upon completion of the drilling, the three in-plane components of residual stress are determined as functions of depth from the surface using the inverse analysis described in ASTM E837. A mean and standard deviation of residual stress along the sample length are calculated from the hole-drilling results at depths between 0.25 mm and 0.75 mm. The hole-drilling mean stress at the top and bottom surfaces of A00 indicate the symmetry of the stress state in the samples and complement the contour data, which tend to be less precise near the measurement plane boundaries [4, 7].

Neutron diffraction planning measurements are made in A08 using the NRSF2 instrument at Oak Ridge National Laboratory. A detailed description of the instrument, data collection, and data analysis can be found elsewhere in the literature [12, 13]. Single-peak diffraction data for the {311} planes are recorded. Three line-scans of strain along the  $Y$  direction are performed at  $X = 8, 12,$  and  $16.0$  mm using a 3.0 mm cube gage volume. Along the outer two lines ( $X = 8$  and  $16.0$  mm) measurements are performed at 6 locations; along the center line ( $X = 12.0$  mm), 16 measurements are performed. Lattice parameters are determined along three principal sample directions at each measurement location. Stress-free lattice parameter found from a set of 5.0 mm cubes cut from the same bar (and assumed to be stress free), enables calculation of strain; residual stress is calculated from the strains using Hooke's law

$$\sigma_i = \frac{E}{(1 + \nu)(1 - 2\nu)} \left( (1 - \nu)\epsilon_i + \nu(\epsilon_j + \epsilon_k) \right); i, j, k \in X, Y \quad (1)$$

with values of elastic properties ( $E$  and  $\nu$ ) as stated above.

## Problem Statement

A problem statement is provided to participants in a series of documents (slides and supporting files). The sample geometry is described in a two-dimensional drawing Fig. 1 and solid part file. The cut plane, A-A, is identified in the drawings as the midplane of the long sample dimension. The problem

statement and sample markings provide a sample number, orientation, fixed coordinate system, and distinct marks on each side of the cut plane; the elastic properties listed above are provided for use in stress calculation. A predetermined cutting configuration describes the EDM setup with a stated wire running direction along the sample  $X$  coordinate and corresponding feed direction along the sample  $Y$  coordinate beginning from  $Y = 0$  mm (cut start) as shown in Fig. 1. Participants are instructed to report residual stress normal to plane A-A as determined by following their typical practice for contour measurements. Participants provide data in triples of  $X$  position in mm,  $Y$  position in mm, and stress in MPa in a text file named according to the sample number. No participant information is to be supplied in the text file. To obscure information in the file, the text file is placed inside two encrypted (password protected) ZIP archives, each with a generic name "stress\_result.zip". Each participant sends a result file to the collector, who is unaware of the ZIP password and the sample identification encoded in the encrypted file.

## Documentation of Practice

Participants are asked to respond to a questionnaire to document basic parameters related to EDM cutting, topography measurement, and analysis procedures, but responses to all queries are optional. Related to cutting, participants provide the EDM wire diameter and whether filler (sacrificial) material [10] is used during cutting. Related to topography measurement, type of measurement system is provided. Related to surface data analysis, participants are asked for a general description of the surface data processing, how outlying surface data are handled. For residual stress calculation, participants are asked for the software used, the type of elements used, the number of elements in the analysis, and the number of elements on the cut plane.

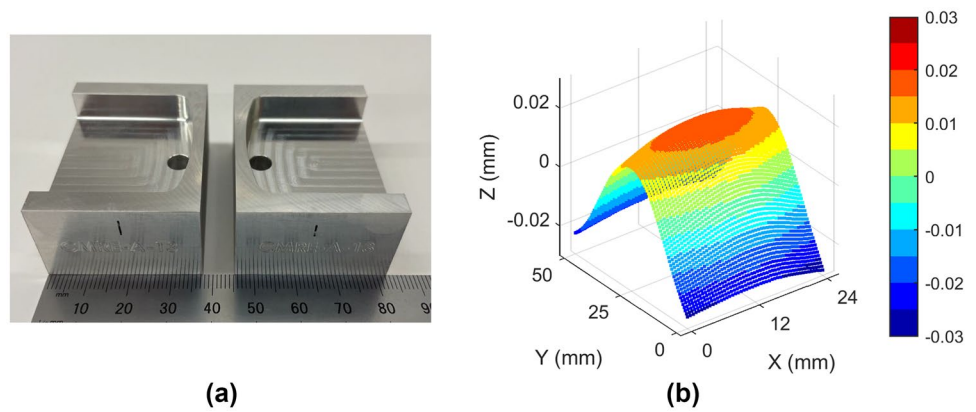
## Analysis of Submissions

The analyst compares participant submissions in various ways, including using color contour plots and line plots through areas of interest. The local maxima on each side (lower and upper) of the axis of the cross-drilled hole are determined and their locations is reported. The average stress reported in the areas of peak tension is also computed. Outlying data are identified using the plots described above, and, if needed, outlying results are set aside.

Reproducibility metrics are computed from non-outlying participant data on a fixed grid with 0.5 mm spacing along both in-plane directions,  $X$  and  $Y$ , to which each participant submission is interpolated. A group mean stress field is computed by averaging all non-outlying submissions at each grid location. Differences between each non-outlying result and the group mean show how the submissions vary



**Fig. 2** Planning measurements: (a) photo of sample A13 following EDM cutting and (b) displacement boundary conditions used in stress analysis for A01



from one another. Maximum and root-mean-square (RMS) of the differences across all grid locations provide metrics to compare among submissions. The observed reproducibility standard deviation is calculated as the sample standard deviation of non-outlying results at each grid location. The average reproducibility across all grid locations provides a single reproducibility metric. Since earlier work has shown lower precision for points near the measurement plane boundaries [5], the average reproducibility standard deviation is also calculated for grid points within 1.0 mm of the boundaries and for interior points (farther than 1.0 mm from the boundaries).

## Results

### Planning Measurements

Planning measurement details describe typical practice used by the fabricator (and in participant measurements).

Sample A13 is pictured in Fig. 2(a) following EDM cutting for the planning measurement. The boundary conditions (derived from surface topography data) and used to compute residual stress for sample A01 are shown in Fig. 2(b).

Results of the planning contour measurements (Fig. 3) demonstrate the spatial distribution of residual stress expected from participants (note: participants are blind to the planning results). Two tensile peaks in the measurement plane above and below the axis of the cross-drilled hole at  $Y = 25.0$  mm are balanced by compressive residual stress at the top and bottom of the plane. The areas not supported by the I-beam web behind the measurement plane have relatively low residual stress. The magnitudes of A01 and A07 are nearly identical, while the magnitude of A13 is somewhat higher. The higher stress in A13 is consistent with that sample being closer to the end of the parent bar than A01 (100.0 mm versus 170.0 mm). Prior work shows elevated stress close to the end of a replicate quenched bar [9]. The residual stress fields for samples

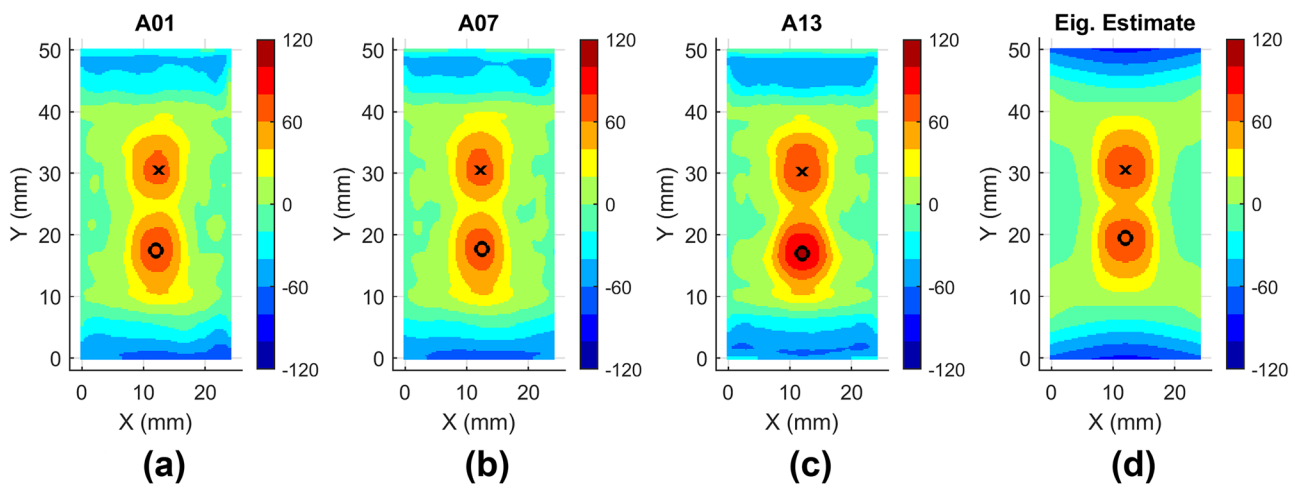


**Fig. 3** Planning measurements: results of contour measurements in (a) A01, (b) A07, and (c) A13 (color scale in MPa)



A01, A00, and A13 are similar to the FE estimate residual stress used in sample design (Fig. 3(d)). An expected stress result is derived by computing the average of results for A01 and A07; the absolute value of differences for the two measurements in Fig. 4(b) shows the largest differences are within 1.0 mm of the plane boundaries. The RMS of differences is 2.7 MPa for all locations on the measurement plane and 5.0 MPa for locations within 1.0 mm of the plane boundaries. Residual stress along the vertical line at  $X = 12.0$  mm is compared in Fig. 5 for contour on A01 and A07, for neutron diffraction (ND) on A08, and hole-drilling on A00. There is excellent agreement in trends. ND data fall above contour by roughly 25 MPa at all locations, which may be due to imprecision in stress-free lattice spacing or discrepancy between the macroscopic stress state and single-peak {311} diffraction; the 25 MPa discrepancy corresponds to  $35 \mu\epsilon$  (assuming uniaxial stress), which is well below the typical instrument uncertainty of 100 – 150  $\mu\epsilon$  [12]. The hole-drilling (HD) results show a symmetric stress field, with nearly identical residual stress at  $Y = 0.5$  and 49.5 mm; HD, contour and ND data are consistent at  $Y = 49.5$  mm, while contour diverges from ND and HD at  $Y = 0.5$  mm. Overall, the planning measurement results give confidence that the sample population is suitable for the reproducibility study, with residual stresses being as expected and similar across samples.

## Documentation of Practice

The participant questionnaire responses are summarized to describe the range of techniques applied by participants.

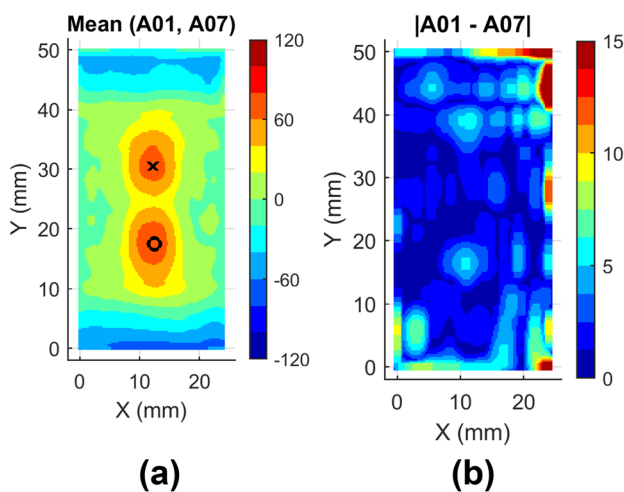


**Fig. 4** Planning measurements: (a) average of stress measured in A01 and A07, and (b) absolute values of differences between stress measured in A01 and A07 (color scale in MPa)

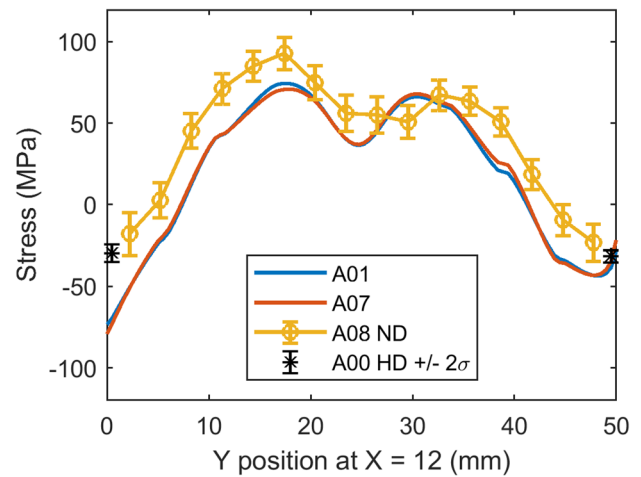


**Fig. 5** Planning measurements: residual stress along  $X = 12.0$  mm for contour measurements in A01 and A07, neutron diffraction measurements in A08, and hole-drilling measurements in A00

The responses are coded separately from the stress results, using randomly assigned participant codes 1 through 8. EDM cutting is documented in Table 1. EDM wire sizes range from 0.1 to 0.25 mm with the most common size 0.25 mm. Three of the eight participants describe using filler (sacrificial) material (ostensibly for similar reasons it was used by the fabricator in the planning measurements): two using it on the wire entry/exit surfaces ( $X = 0.0$  mm and  $X = 24.0$  mm) and one using it on the cut start/stop ( $Y = 0.0$  mm and  $Y = 50.0$  mm).

The surface topography measurement and data processing steps are described in Table 2. Metrology equipment employs a mix of contact (touch probe) and non-contact (laser) technologies. Most participants use visual inspection to handle outliers, and some employ other techniques. The most common surface fitting technique is bivariate spline fitting.

**Table 1** Summary of participant responses to questions regarding cutting (– indicates no response)

Participant	EDM Wire Used	Filler Material
1	0.25 mm	2 mm aluminum plates (cut start/stop)
2	0.1 mm	Top and bottom (wire entry/exit)
3	0.25 mm	12.7 mm aluminum clamp with pilot hole (cut start/stop)
4	0.15 mm	–
5	0.25 mm	None
6	0.20 mm	None
7	0.15 mm	–
8	0.25 mm	None



**Table 2** Summary of participant responses to questions regarding topography smoothing or fitting (– indicates no response)

Participant	Type of measurement system	Outlier handling	Type of fitting used
1	Confocal interferometer	Threshold and visual	Splines
2	Hybrid CMM with touch-probe for perimeter and alignment and laser triangulation probe for surface topography	Median filtering and visual inspection	Local polynomial fitting
3	Tactile CMM	Visual	Bi-variate spline fitting in Matlab
4	Chromatic white light interferometer	Visual	Bi-variate splines
5	Laser interferometer	Alpha-shape algorithm, visual	Splines
6	Tactile CMM	Visual	Splines
7	Tactile CMM	Visual	Splines
8	Laser interferometer	–	–

Table 3 summarizes the residual stress calculation steps. Most participants perform analysis in ABAQUS with 200,000 to 300,000 elements. One participant used Stress-Check, a so-called p-code that uses large size elements, each having high-order displacement interpolation.

**Analysis of Submissions**

Contour plots of residual stress reported by each participant are shown in Fig. 6. Overall, the participant results have similar trends to the planning measurements, with two tensile peaks above and below the axis of the cross-drilled holes and compression near the top and bottom edges. Two results are identified as outliers, A06 and A11, given their basic appearance in Fig. 6. The locations of the interior peak tension above and below the axis of the cross-drilled holes (at Y = 25.0 mm) are identified by symbols (x and o) in Fig. 6, with the precise locations and values of peak stress listed in Table 4. Excepting the two outliers, participants identify the peak tensions at the mid-width, near X = 12.0 mm at heights near Y = 20.0 mm (lower peak) and Y = 30.0 mm (upper peak). Most participants’ results have the peak tension below the cross drilled holes at the lower location,

near Y = 20.0 mm, but A10 and A09 report the opposite trend. To compare the tensile peak magnitudes, the average stress is calculated for locations within a 3 mm radius of X = 12.0 mm, and Y = 20.0 mm or Y = 30.0 mm (i.e., near the lower or upper peak, respectively). Data in Fig. 7 and Table 4 show that there is less difference between the residual stress near upper and lower near-peak tensile regions than indicated by the single peak values. The two outliers, A06 and A11, have locations of peak stress and values of maximum tensile stress that are quite different than found other samples (Fig. 6, Table 4). Similarly, the average residual stress near the expected locations of peak tension for A06 and A11 are outliers (Fig. 7, Table 4).

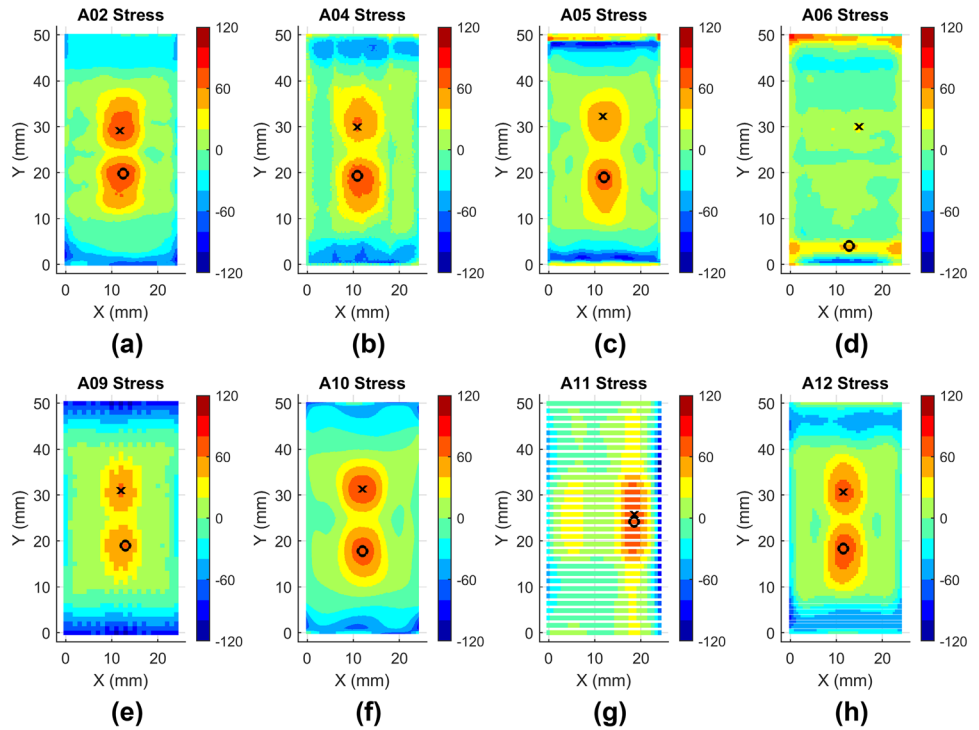
Figure 8 shows the group mean and reproducibility standard deviation computed from the six non-outlying results. The lower and upper peak tensions in the group mean of Fig. 8 are 68.7 and 64.2 MPa, respectively (also shown in Table 4) and the stress field ranges from roughly -60 to 70 MPa. The reproducibility standard deviation in Fig. 8(b and c) has the largest values at the bottom (Y = 0 mm) and top (Y = 50.0 mm) plane boundaries. Elevated reproducibility standard deviation values are also present at the left (X = 0 mm) and right (X = 24.0 mm) boundaries. The reproducibility standard deviation ranges

**Table 3** Summary of participant responses to questions regarding residual stress calculation (– indicates no response)

Participant	Software used	Element type	Number of elements	
			In model	On cut plane
1	In house program	-	300,000	–
2	Abaqus 2018	C3D8R	–	–
3	Abaqus	C3D8R	208,656	4,800
4	Abaqus	C3D10	358,148	15,920
5	Abaqus	C3D10	289,208	27,246
6	Abaqus	C3D10	334,874	–
7	ERSD StressCheck	8th order hexahedral	63	9
8	Abaqus	-	–	–



**Fig. 6** Residual stress reported by each participant (markers o and x show locations of peak stress; differences of plot appearance reflect differences among point spacings of data provided by participants; color scale in MPa)



from 0.5 to 54.8 MPa with an average of 8.1 MPa on the plane. At locations within 1.0 mm of the boundaries, the average reproducibility standard deviation is about 3 times higher when compared to locations farther than 1.0 mm of the boundary (17.6 versus 6.1 MPa).

Line plots in Fig. 9 report the six non-outlying participant results along the two bisectors of plane A-A. Data along  $X = 12.0$  mm (Fig. 9(a)) have similar trends for all samples except near the bottom ( $Y = 0$  mm) and top ( $Y = 50.0$  mm) where there is significant scatter. The HD results for sample A00 agree well with the contour group mean near the bottom and top surfaces (Fig. 9(a)). Results for samples A04 and A10 are quite similar to the group mean and to the HD data. Data along  $Y = 25.0$  mm (Fig. 9(b)), between the tensile peaks, show a lower

magnitude of residual stress and smaller values of reproducibility standard deviation. There is larger scatter in measurements near the plane boundaries ( $X = 0$  and  $24.0$  mm).

Contour maps of the differences between non-outlier results and the group mean are plotted in Fig. 10. For all samples, the largest differences are near the measurement plane boundaries. Near  $Y = 0$ , where the prescribed EDM cutting begins and near  $Y = 50.0$  mm, where the EDM cutting ends, the differences are elevated and without a clear trend. The RMS difference for each sample ranges from 7.8 to 14.1 MPa (Fig. 11), while the maximum differences range from 35.5 to 107 MPa. Samples exhibiting the largest maximum difference also exhibit the largest RMS difference. Residual stress in four of the six samples have very similar RMS differences (8 to 9 MPa).

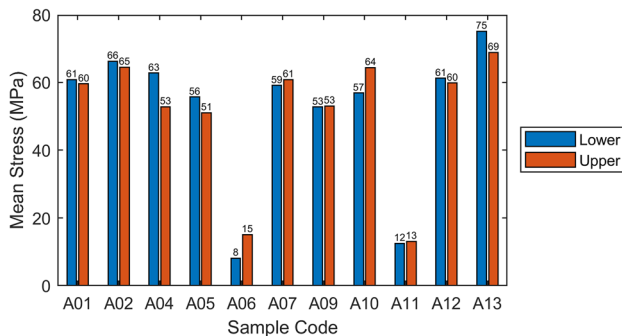


**Fig. 7** Mean stress near lower and upper tensile peaks for all samples

## Discussion

### Outliers

Noteworthy methodological errors were determined to cause the outlying results for A06 and A11. The specific errors were determined via anonymized dialogs between the analyst and the specific participants, anonymity provided by passing communications and files through the distributor. The communications included an exchange of surface topography data, comprising the participant





**Table 4** Metrics for peak residual stress from planning (FE estimate, measurements) and participant measurements; italic face indicates outliers A06 and A11

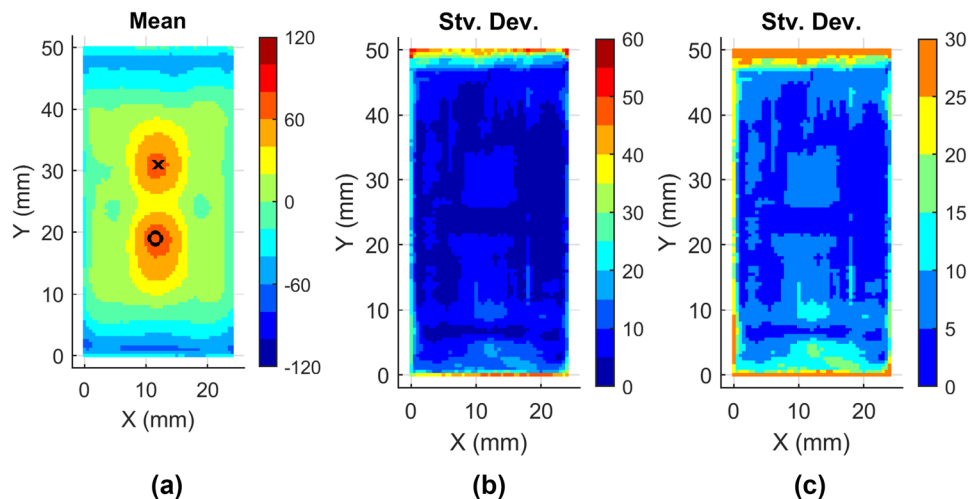
Sample	Lower Peak [o]			Upper Peak [x]			Near-Peak Average	
	X (mm)	Y (mm)	RS (MPa)	X (mm)	Y (mm)	RS (MPa)	Lower (MPa)	Upper (MPa)
<i>Planning</i>								
FE Estimate	12.0	19.5	75.7	12.0	30.5	75.7	68.7	68.7
A01	12.3	17.5	74.5	12.5	30.5	66.6	60.9	59.6
A07	12.5	17.8	71.3	12.3	30.5	68.1	59.1	60.8
A13	12.0	17.0	101.9	12.0	30.3	76.7	75.1	68.9
<i>Participant Measurements</i>								
A02	12.5	19.8	78.3	11.7	29.2	72.5	66.3	64.5
A04	10.9	19.3	76.7	10.9	29.9	63.4	62.8	52.8
A05	12.0	19.0	66.1	11.8	32.3	58.4	55.7	51.1
A09	13.0	19.0	60.1	12.0	31.0	62.0	52.8	53.1
A10	12.0	17.8	69.3	12.0	31.3	75.6	56.9	64.4
A12	11.5	18.4	71.3	11.5	30.7	67.5	61.3	59.9
Mean (non-outliers)	11.5	18.8	68.7	11.5	30.7	64.2	59.3	57.3
A06	<i>12.8</i>	<i>4.0</i>	<i>48.0</i>	<i>15.0</i>	<i>30.0</i>	<i>22.8</i>	<i>8.1</i>	<i>15.1</i>
A11	<i>18.6</i>	<i>24.2</i>	<i>72.4</i>	<i>18.6</i>	<i>25.6</i>	<i>74.5</i>	<i>12.5</i>	<i>13.1</i>

generated data and the boundary conditions used by the analyst to calculate residual stress for A01 (Fig. 2(b)).

While sample A06 was cut along the specified measurement plane, the participant suspected issues with their surface measurement system and subsequently repeated the surface measurements on a new system. The participant computed boundary conditions are significantly different for the original (Fig. 12(a)) and subsequent (Fig. 12(b)) surface measurements. The residual stress computed from the updated boundary conditions in Fig. 12(c) resembles the non-outlying results of Fig. 8(a). The analyst and A06 participant therefore attribute this outlier to an unknown issue with the surface measurement system.

While sample A11 was cut along the specified measurement plane, the participant supplied surface topography data for each side of the cut (Fig. 13(a) through (d)) show an unexpected feature. The surface topography are mildly asymmetric when looking along the Y axis in Fig. 13(b) and (d), and a significant cutting artifact is present for X > 20 mm. Exact details of the EDM cutting were not available, and further diagnosis of the EDM cutting problems was not possible. The analyst processed the surface topography data to develop an updated boundary condition (Fig. 13(e)) and stress result (Fig. 13(f)). The new stress result (developed by the analyst) contains the expected tensile peaks adjacent to the axis of the cross-drilled hole; however, the result also contains a tensile

**Fig. 8** Maps of (a) the mean residual stress for all non-outlying submissions, (b) the reproducibility standard deviation, and (c) the reproducibility standard deviation on a reduced color scale (color scale in MPa)



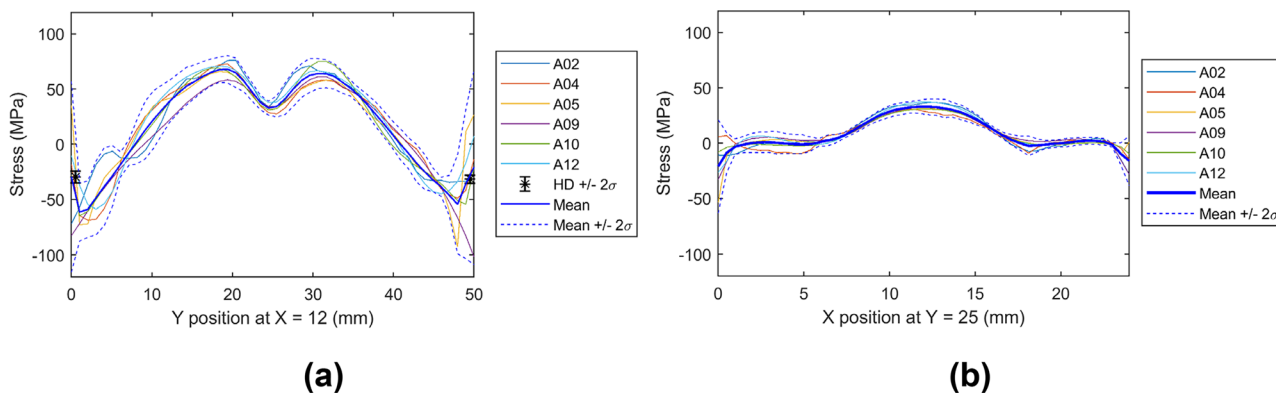
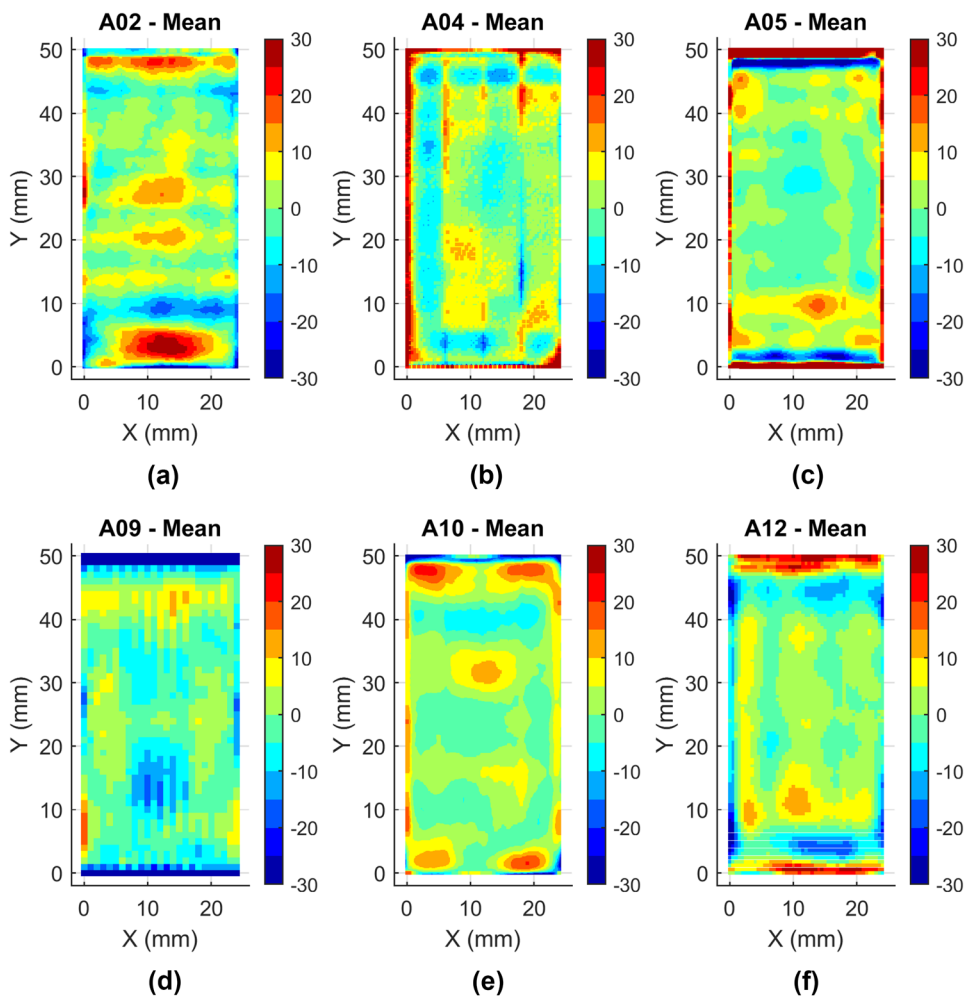


**Fig. 9** Line plots of non-outlying contour method data along (a) X = 12.0 mm and (b) Y = 25.0 mm with mean and 2-sigma bounds indicated; symbols in (a) show results of hole-drilling measurements

peak along X = 19.0 mm that is consistent with a wire break or similar EDM artifact. Communication with the participant revealed that their stress calculation approach simplified the out-of-plane sample geometry to a prismatic block, without

capturing the I-beam cross-section or cross-drilled holes. The analyst and A11 participant therefore attribute this outlier to a cutting artifact and an over-simplified out-of-plane geometry in the residual stress calculation.

**Fig. 10** Maps of absolute differences in stress between each non-outlying measurement and the mean of non-outlying measurements (color scale in MPa)



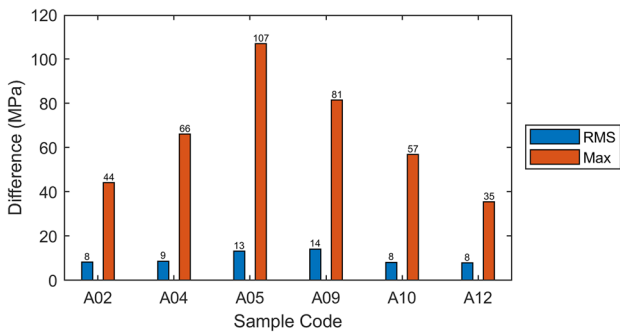


Fig. 11 Difference statistics for non-outlying results

### Significance of Results

The interlaboratory reproducibility standard deviation found here agrees well with the intralaboratory repeatability observed previously. Olson et al. [5] reported average repeatability standard deviation divided by elastic modulus as 125 parts-per-million for points in the measurement plane interior and 250 parts-per-million for points within 1.0 mm of the boundary. For the aluminum in the present study, with  $E = 71.7$  GPa, the corresponding repeatability standard deviation is 9.0 MPa in the interior and 18 MPa near the boundary. These values compare well to the average reproducibility standard deviation found here: 6.1 MPa for locations away from the plane boundaries and 17.6 MPa for locations within 1.0 mm of the plane boundaries.

The results of this study are also similar to the reproducibility standard deviation reported in the prior study

on data analysis [7], which included many of the same participants. The prior study assumed a similar material, but the stress distribution was larger, with 130 MPa peak magnitude. In the present study, the overall reproducibility standard deviation is low ( $< 5$  MPa) over much of the cross-section and higher near the boundaries (15–22 MPa). Given the additional scope of this study, including fabrication of physical samples, EDM cutting, and surface topography measurement, the similar level of reproducibility standard deviation is somewhat unexpected. Increased measurement dispersion had been expected because of variability in each of the physical operations performed by the participants as well as differences in practice.

The planning measurements demonstrate repeatability of the fabricated samples and the residual stress state. Consistency between the planning measurements and the non-outlying participant results indicate the samples contain a repeatable stress state and the contour method has a high degree of reproducibility. Although the participants use various cutting configurations, measurement instruments, and finite element analyses, the robustness of the contour method yields reproducibility consistent with previously estimates of repeatability for the sample configuration considered.

Additional work to assess contour method reproducibility is being actively considered by the present authors. Future work that focuses on one of the contour method measurement steps, such as cutting or topography measurement, might reveal underlying sources of uncertainty and present opportunities for improvement.

Fig. 12 Displacement boundary conditions (a) used in original submission for A06 and (b) determined from new measurement data (note difference in z axis scale for a and b); (c) revised residual stress (color scale in MPa)

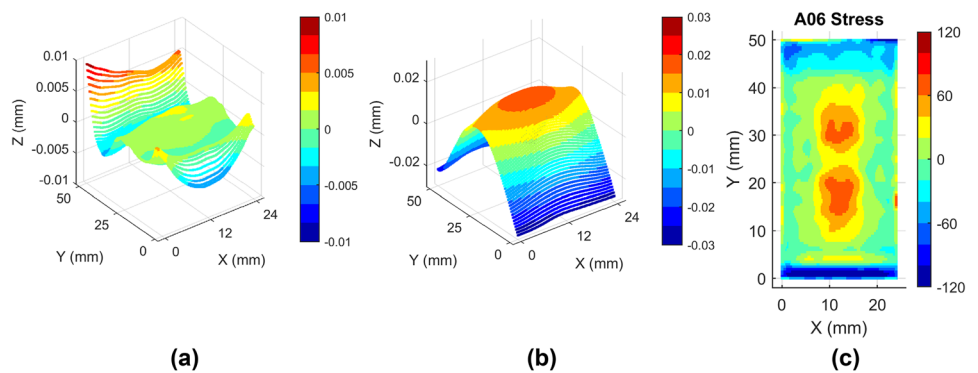
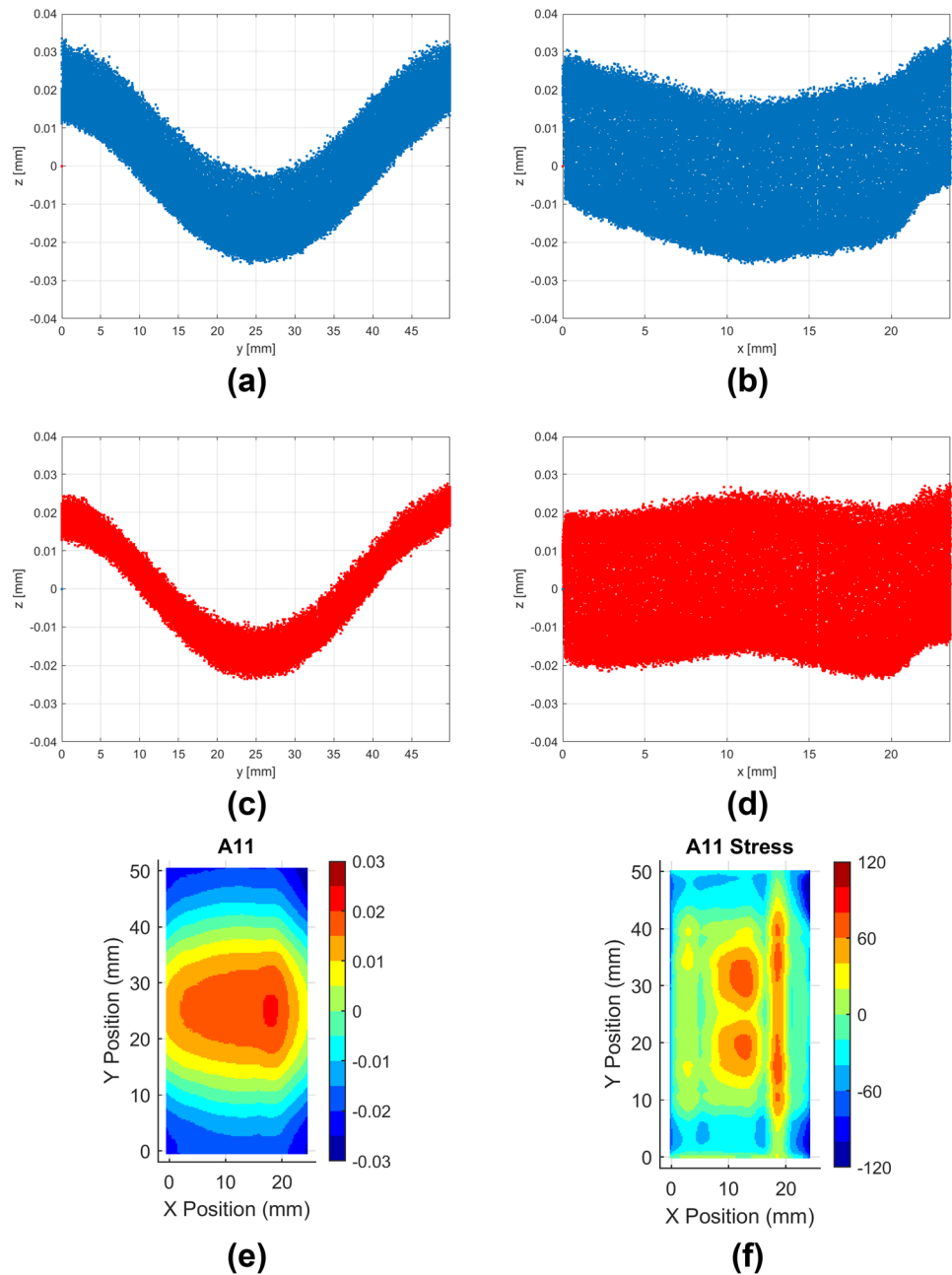


**Fig. 13** Surface topography for A11: side 1 viewed along (a) X and (b) Y, side 2 viewed along (c) Y and (d) X, (e) boundary condition developed by analyst (color scale in mm), and (f) residual stress computed with accurate sample geometry (color scale in MPa)



## Conclusions

The paper reports results of a contour method reproducibility study, spanning the complete contour measurement process. Fourteen identically prepared samples are extracted from a single residual stress bearing bar. Eight are distributed to a group of participants in a double-blind reproducibility experiment. Five samples are used for planning measurements with complementary techniques comprising contour method, hole-drilling, and neutron diffraction. Planning

measurements show a residual stress state useful for assessing reproducibility, both in terms of the residual stress field to be measured and the consistency of stress among samples allocated to participants. Eight participants completed contour method residual stress measurements. Two results were identified as outliers and set aside; the root causes for the outlying results were found to be errors with procedures and equipment. The six non-outlying results are used to calculate a distribution of reproducibility standard deviation on the measurement plane. The observed reproducibility standard



deviation ranged from 0.5 MPa to 54.8 MPa and averaged 8.1 MPa for all locations on the measurement plane. The reproducibility standard deviation is 6.1 MPa for locations away from the plane boundaries and 17.6 MPa for locations within 1.0 mm of the plane boundaries. These values of average interlaboratory reproducibility standard deviation are similar to values of intralaboratory repeatability standard deviation reported previously.

**Acknowledgements** The authors would like to acknowledge Jeffrey Bunch for his meticulous efforts in maintaining the integrity of the double-blind study as the *distributor* and *collector*. His review of the work offered the group excellent insights from his many years in the aircraft industry. The authors would like to acknowledge Jeffrey Bunn for enabling the neutron diffraction work on the NRSF2 instrument at ORNL. A portion of this research used resources at the High Flux Isotope Reactor, a DOE Office of Science User Facility operated by the Oak Ridge National Laboratory. The authors express their gratitude to all the specialized EDM technicians who enabled the contour cuts.

**Funding** This study was performed by the authors without the support of external funding.

## Declarations

**Disclosure of Potential Conflicts of Interest** CRD is a graduate student pursuing a doctorate under the guidance of MRH. JAO, BTW, and MRH have separate economic interests in contour method measurements that derive from their employment by (JAO and BTW) or an ownership interest in (MRH, Hill Engineering, LLC of Rancho Cordova, CA, USA) a firm providing contour method measurements. The remaining authors report no conflicts of interest.

**Open Access** This article is licensed under a Creative Commons Attribution 4.0 International License, which permits use, sharing, adaptation, distribution and reproduction in any medium or format, as long as you give appropriate credit to the original author(s) and the source, provide a link to the Creative Commons licence, and indicate if changes were made. The images or other third party material in this article are included in the article's Creative Commons licence, unless indicated otherwise in a credit line to the material. If material is not included in the article's Creative Commons licence and your intended use is not permitted by statutory regulation or exceeds the permitted use, you will need to obtain permission directly from the copyright holder. To view a copy of this licence, visit <http://creativecommons.org/licenses/by/4.0/>.

## References

1. Prime MB (2001) Cross-Sectional Mapping of Residual Stresses by Measuring the Surface Contour after a Cut. *J Eng Mater Technol* 123:162–168
2. Prime MB, DeWald AT (2013) The Contour Method. In: Schajer, G.S., ed. *Practical Residual Stress Measurement Methods*, West Sussex John Wiley & Sons West Sussex.
3. Prime MB (2022) Contour Method: Publications and Preprints. <https://www.lanl.gov/contour/pubs.html> (retrieved Jan 15, 2022).
4. Hill MR, Olson MD (2014) Repeatability of the Contour Method for Residual Stress Measurement. *Exp Mech* 54(7):1269–1277
5. Olson MD, DeWald AT, Hill MR (2018) Repeatability of contour method residual stress measurements for a range of materials, processes, and geometries. *Materials Performance and Characterization* 7(4):20170044–20170044. <https://doi.org/10.1520/MPC20170044>
6. Olson MD, DeWald AT, Prime MB, Hill MR (2014) Estimation of Uncertainty for Contour Method Residual Stress Measurements. *Exp Mech* 55(3):577–585
7. D'Elia CR, Carlson SS, Stanfield ML et al (2020) Interlaboratory Reproducibility of Contour Method Data Analysis and Residual Stress Calculation. *Exp Mech* 60:833–845. <https://doi.org/10.1007/s11340-020-00599-0>
8. Hosseinzadeh F, Kowal J, Bourchard PJ (2014) Towards Good Practice Guidelines for the Contour Method of Residual Stress Measurement. *J Eng* 8:453–468
9. Olson MD, Hill MR (2015) A New Mechanical Method for Biaxial Residual Stress Mapping. *Exp Mech* 55:1139–1150. <https://doi.org/10.1007/s11340-015-0013-5>
10. Hosseinzadeh F, Ledgard P, Bouchard PJ (2013) Controlling the Cut in Contour Residual Stress Measurements of Electron Beam Welded Ti-6Al-4V Alloy Plates. *Exp Mech* 53:829–839. <https://doi.org/10.1007/s11340-012-9686-1>
11. ASTM International (2021) E837–20 Standard Test Method for Determining Residual Stresses by the Hole-Drilling Strain-Gage Method. West Conshohocken, PA: ASTM International
12. Cornwell P, Bunn J, Fancher CM, Payzant EA, Hubbard CR (2018) Current capabilities of the residual stress diffractometer at the high flux isotope reactor. *Rev Sci Instrum* 89(9):092804. <https://doi.org/10.1063/1.5037593>
13. Fancher CM, Bunn JR, Bilheux J, Zhou W, Whitfield RE, Borroguero J, Peterson PF (2021) pyRS: a user-friendly package for the reduction and analysis of neutron diffraction data measured at the High Intensity Diffractometer for Residual Stress Analysis. *J Appl Crystallogr* 54(6):1886–1893. <https://doi.org/10.1107/S1600576721010554>

**Publisher's Note** Springer Nature remains neutral with regard to jurisdictional claims in published maps and institutional affiliations.

